ORIGINAL PAPER

Electrocatalytic activities of Nafion/CdSe/Self-doped polyaniline composites to dopamine, uric acid, and ascorbic acid

Yeong-Tarng Shieh · Yi-Ting Lu · Tzong-Liu Wang ·
Chien-Hsin Yang · Rong-Hsien Lin

Abstract Composites of Nafion, COOH-capped CdSe, and self-doped polyaniline (SPAN) were used to prepare novel chemical modified glassy carbon electrodes (Nafion/CdSe/SPAN/GCE). The electrocatalytic activities of the modified GCE to the redox reactions of dopamine (DA), uric acid (UA), and ascorbic acid (AA) were investigated by cyclic voltammetry (CV). CV curves revealed that the electrocatalytic activities of Nafion/CdSe/SPAN/GCE to oxidations of the analytes in solution of pH 7 were in the order of DA>UA>AA. This order was consistent with the strong-to-low extent of interactions between the modified GCE and the analytes. These interactions were consistent with the observations that the oxidation rate of DA followed a diffusion-controlled process whereas that of UA followed a surface adsorption-controlled process. The composites of casting at higher pH levels were found to exhibit better CdSe and SPAN dispersions in films and higher electrocatalytic activities. CdSe and SPAN exhibited insignificant synergistic effects on the oxidations of DA when cast from Nafion solutions of both low and high pHs whereas CdSe and SPAN exhibited much synergistic effects on the oxidations of UA when cast from the Nafion solution of high pH at 12.

Keywords Self-doped polyaniline · CdSe · Nafion · Electrocatalytic activity · Cyclic voltammetry

Y.-T. Shieh (✉) · Y.-T. Lu · T.-L. Wang · C.-H. Yang
Department of Chemical and Materials Engineering,
National University of Kaohsiung, Kaohsiung 811, Taiwan
e-mail: yts@nuk.edu.tw

Y.-T. Lu · R.-H. Lin
Department of Chemical and Materials Engineering, National
Kaohsiung University of Applied Sciences, Kaohsiung 807, Taiwan

Introduction

The rapid and accurate determination of dopamine (DA) concentration in body fluid is important to diagnose schizophrenia and Parkinson's disease. Ascorbic acid (AA) largely coexists with DA in the body fluid. Since the oxidation potential of AA is similar to that of DA due to homogeneous catalytic effect, it is of importance to distinguish DA from AA or eliminate the interference of AA during the detection of DA. Uric acid (UA) is main final products of purine metabolism in the human body. UA and AA coexist in blood and urine. It is not easy to selectively detect UA in the presence of AA, due to similar oxidation potentials of UA and AA at bare electrodes. There have been many investigations in the development of methods for the selective detections of DA, UA, and AA via modifications of the working electrodes [1–14]. In previous studies [15, 16], interactions between temperature-responsive modified electrodes and the three analytes were varied with temperature so that different extents of interactions between the modified electrodes and the analytes could be obtained by varying temperature to achieve the selective detection ability for the three analytes. One of the interactions for achieving selective detection abilities for a mixture of analytes can be the ionic interaction which is demonstrated in this study.

To increase the electrocatalytic activity of a modified working electrode, conducting polymers have reportedly been used to modify electrodes [17–22]. For this goal, self-doped conducting polyanilines (SPAN) were previously prepared by the method of cyclic voltammetry (CV) on indium tin oxide (ITO) electrodes in aniline (AN) and o-aminobenzene sulfonic acid (OSA) mixed monomer solutions to obtain SPAN-modified ITO electrodes [23, 24]. The electrocatalytic activity of the SPAN to the $Fe(CN)_6^{3-/4-}$ probe, a redox couple, was significantly pH-dependent. In this study, SPAN was prepared by the chemical oxidation polymerization of AN

in HCl aqueous solution to obtain polyaniline emeraldine salt (ES), followed by sulfonation of the de-doped emeraldine base (EB) to obtain the self-doped sulfonated polyaniline.

Nanoparticles have been employed as modifiers in the fabrication of chemically modified electrodes [25–27]. Carbon nanotubes (CNT), for example, reportedly exhibited good electrocatalytic activities [28–34] ascribed to the porous characteristic of CNT films on the surfaces of electrodes that exhibited a "thin film" effect leading to the enhanced currents and/or lowered potentials [35–37]. The CdSe colloidal quantum dots are II–VI semiconductor nanoparticles and exhibit unique size-dependent optical properties and are of great interest for applications in optoelectronic and photovoltaic devices. CdSe/ZnS quantum dots were reportedly used as a sensitive "indicator" for glucose analysis [38]. In this study, water-soluble COOH-capped CdSe quantum dots were synthesized by an aqueous process and were investigated as semiconductor nanoparticles on their electrocatalytic properties. For the goal of developing a selective sensor, the composites of SPAN, COOH-capped CdSe, and a commercial available Nafion solution were used to modify glassy carbon electrode (GCE) to investigate interactions between the modified electrodes and the three analytes described above and correlate these interactions with the electrocatalytic activities of the modified electrodes to the three analytes in this study.

Experimental

Preparation of hydrophilic COOH-capped CdSe powders

Sodium selenosulfate (Na$_2$SeSO$_3$) was first produced by reacting sodium sulfite (Na$_2$SO$_3$, reagent grade, 98 % purity, supplied by Aldrich) with selenium (Se, 99.5 % purity, supplied by Aldrich) powders at a mole ratio of 3/1. In a typical experiment, a 50-ml deionized water was first heated at 90 °C in N$_2$ for 30 min with constant stirring, followed by the additions of 3.78 g of sodium sulfite (0.6 M) and 0.79 g of Se (0.01 mol) powders. The solution was refluxed for about 3.5 h allowing the solution to become clear to obtain sodium selenosulfate. After cooling down to room temperature and filtration, the clear sodium selenosulfate solution was stored in the dark for the preparation of the hydrophilic COOH-capped CdSe powder. In the experiment, a 150-ml deionized water was heated at 90°C in N$_2$ for 30 min, followed by the additions of 0.24 g of CdCl$_2$ (98 % purity; Sigma-Aldrich) and 3.3 ml of mercaptoacetic acid (MAA, 98 % purity, Aldrich) aqueous solution (1 M) under stirring in N$_2$ for 3 h, followed by adding NaOH solution (1 M) to adjust pH to 11 at which 3.3 ml of the sodium selenosulfate solution was added and kept stirring for 20 min to obtain a yellow solution. A 300-ml methanol was added to precipitate the COOH-capped CdSe, followed by centrifuging at 6,000 rpm for 15 min to collect the COOH-

capped CdSe. The COOH-capped CdSe powders can be obtained after drying in a vacuum oven at room temperature. The so-prepared COOH-capped CdSe powders were water soluble. Without mercaptoacetic acid added in the final stage of the CdSe preparations, the CdSe nanoparticles were found to settle down in water and the dried CdSe powders could not dissolve in water. Ultraviolet–visible (UV–Vis) spectrophotometer (Perkin-Elmer Lambda 35) was used to determine the particle size of the CdSe colloid in solution. The particle size was determined to be 2.4 nm.

Preparations of SPAN

Polyaniline (PANI) was synthesized via the chemical oxidation method. In a typical experiment, 2.421 g of AN was dissolved in 1.2 M HCl aqueous solution, followed by adding 6.1484 g of ammonium persulfate under N$_2$ with constant stirring in an ice bath for 3 h. The reacted mixture was filtered to remove unreacted AN by washing with the HCl aqueous solution. The obtained ES form of PANI was then soaked in 1 M ammonium aqueous solution for 1 day to obtain the dedoped PANI EB form. It was then converted to SPAN by sulfonation of the EB. The EB (0.5 g) was sulfonated by dissolving in 40 ml of fuming sulfonic acid with constant stirring in an ice bath for 2 h. The resulting dark purple solution was then precipitated with 200 ml methanol followed by 100-ml acetone, the temperature being held between 10 °C and 20 °C by an ice bath. The precipitate was then washed by a large amount of methanol until the filtrate had a pH of 7. The product was vacuum-dried at room temperature for 24 h to obtain SPAN. UV–Vis spectrophotometer (Perkin-Elmer Lambda 35) was used to analyze the formation of SPAN.

Preparations of Nafion/CdSe/SPAN dispersions

A 40 μl of 5 wt.% Nafion solution (perfluorinated resin solution in lower aliphatic alcohols and water, supplied by Aldrich) was added into 1 ml of deionized water to prepare a solution containing 0.2 wt.% Nafion. One milligram of the hydrophilic COOH-capped CdSe powder and one mg of SPAN were then added into the Nafion solution. The Nafion/CdSe/SPAN dispersion having a pH between 4 and 5 can be obtained after 10 min of sonication. Without the addition of CdSe or SPAN, the dispersion of Nafion/SPAN or Nafion/CdSe can also be prepared.

Preparations of Nafion/CdSe/SPAN modified GCE

An amount of 10 μl of the Nafion/CdSe/SPAN dispersion without adjusting its pH was cast on a prepolished GCE to obtain Nafion/CdSe/SPAN/GCE. The cast film was allowed to dry in ambient air. The same amount (10 μl) of Nafion, Nafion/SPAN, and Nafion/CdSe was also cast on the

prepolished GCE to obtain Nafion/GCE, Nafion/SPAN/GCE, and Nafion/CdSe/GCE for comparisons. For the preparations of Nafion-pH/CdSe/SPAN modified GCE, ammonium aqueous solution (0.5 M) and acetic acid aqueous solution (0.5 M) were used to adjust pH of the dispersions to pH 2, 7, or 12 before casting on GCE. Thus, to give two examples, Nafion-12/CdSe/SPAN modified GCE denotes that GCE was cast from the Nafion/CdSe/SPAN dispersion of pH 12. Nafion-2/SPAN modified GCE denotes that GCE was cast from the Nafion/SPAN dispersion of pH 2. Each dispersion was also cast on an ITO glass for analysis of surface morphology of the film using an optical microscopy (OM, Nikon Eclipse LV 100) and a field emission scanning electron microscopy (FESEM; Hitachi S-4800) at an operating voltage of 1 keV.

Electrochemical measurements

A potentiostat (CH611D, CH Instruments) was used to perform CV analyses at 25 °C in a conventional three-electrode system with GCE as working electrode, a platinum wire as auxiliary electrode, and Ag/AgCl/3 M KCl as reference electrode. The phosphate buffer solution (PBS) of pH 7 was used as the background electrolyte in experiments. The modified GCE was immersed in 2 mM DA, UA, or AA (Sigma-Aldrich) in PBS of pH 7 containing 0.1 M KCl to investigate the electrocatalytic activities of the various cast films on GCE. The GCE has a round active area with 3 mm in diameter. CV was conducted between −0.4 and 0.8 V at a scan rate of 50 mV/s. The second CV cycle was used for the investigations on electrocatalytic activities of the films.

Results and discussion

### Characterizations of CdSe and SPAN and their dispersions in Nafion

Figure 1a shows the UV–Vis absorption spectrum of the as-prepared CdSe colloids in water. As can be seen in Fig. 1a, the optical absorption threshold for the CdSe colloids appears at near 508 nm corresponding to the band gap of the CdSe particle. According to Brus's model [39], the excited energy of nanocrystals is in reverse of their particle size. If the excited energy of nanocrystal is higher, the maximum absorption peak of its UV–Vis spectrum is blue-shifted. To obtain a more accurate optical band gap of the CdSe nanoparticles, the fundamental equation $\alpha h\nu = B(h\nu - E_{opt})^n$ developed in the Tauc relation [40] was used, where α is the absorption coefficient, $h\nu$ is the energy of absorbed light, n is equal to 1/2 for the direct allowed transition, and B is the proportionality constant. The optical band gap (E_{opt}) calculated by this equation is 2.55 eV, as shown in Fig. 1b. Based on this band gap,
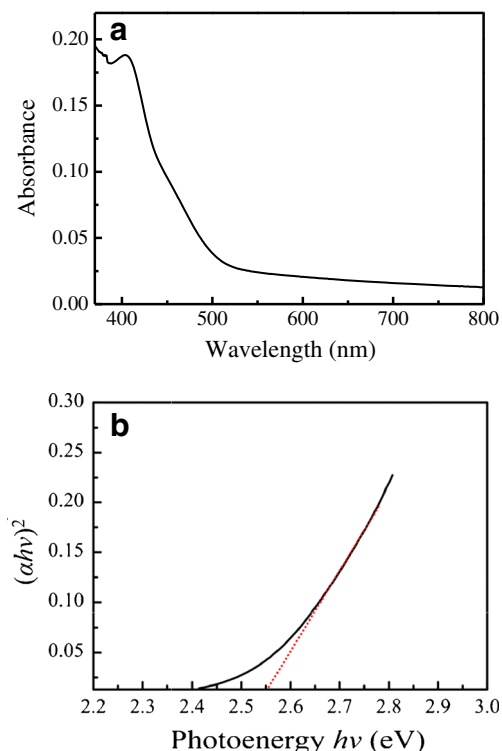
Fig. 1 UV–Vis spectroscopy of **a** the COOH-capped CdSe colloidal aqueous solution and **b** plot of $(\alpha h\nu)^2$ versus $h\nu$ for the COOH-capped CdSe colloids

the estimated size of CdSe nanoparticles was approximately 2.4 nm by the potential morphing method [41].

Figure 2 shows UV–Vis spectra for the three types of PANIs. Spectrum a in Fig. 2 has a peak at near 350 and 450 nm corresponding to π–π^* transition of the benzenoid rings in the PANI and to the polaron band transition in the ES of PANI, respectively [42]. The broad peak centered at near
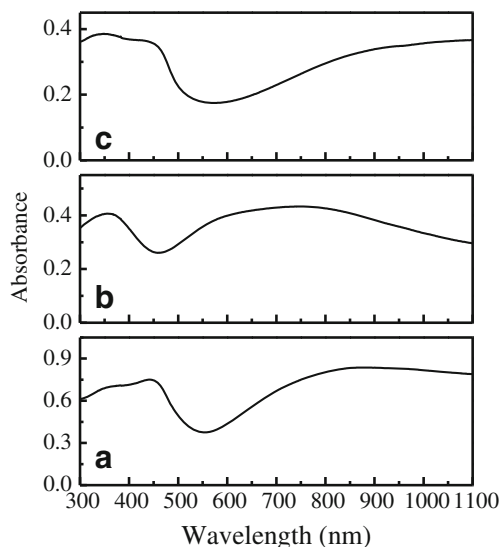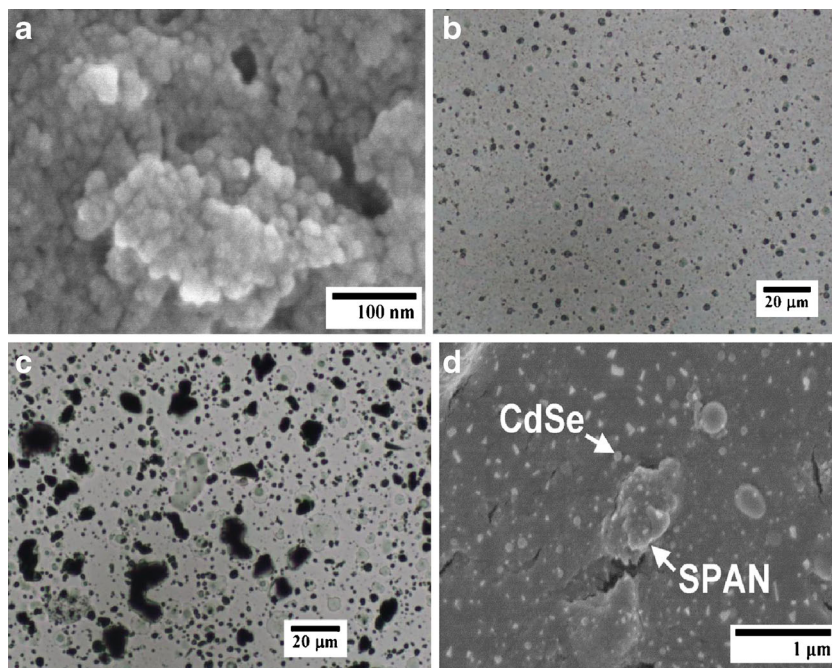

Fig. 2 UV–Vis spectroscopy of various forms of polyanilines: **a** emeraldine salt (*ES*), **b** emeraldine base (*EB*), and **c** sulfonated polyaniline (i.e., self-doped polyaniline [*SPAN*])

900 nm corresponds to the exciton transition of the quinoid rings in the ES form of PANI. After dedoping of the ES by adding ammonium aqueous solution, the absorption at near 450 nm disappeared and the broad peak that centered at near 900 nm blue-shifted to near 700 nm as can be seen in spectrum b of Fig. 2, an indication that the ES form was successfully changed to the EB form in PANI. The broad peak at near 850 nm in spectrum c of Fig. 2 can be assigned to polaron band transitions for the SPAN according to Chen and Hwang [42] who reported that, before neutralization by adding NaOH, the aqueous self-acid-doped sulfonic acid ring-substituted polyaniline (SPAN) in the doped state exhibited absorbance at 830 nm due to polaron band transitions. As the level of neutralization of SPAN was increased, the polaron band disappeared gradually and a strong absorption due to exciton transition of the quinoid rings at 570–600 nm grew at the same time. It was evident from Fig. 2 that SPAN was successfully prepared.

Figure 3 shows OM and FESEM images for the COOH-capped CdSe powders and the cast films of three composites. From the FESEM image in Fig. 3a, the particle size of the CdSe powders was roughly in between 15 and 20 nm, indicating that aggregation of CdSe powders occurred during drying, as compared with 2.4 nm that was determined by the UV–Vis spectroscopy for the CdSe colloids in aqueous solution. The OM image in Fig. 3b showed that CdSe particle was quite uniformly dispersed in Nafion, whereas in Fig. 3c the SPAN appeared to have relatively large aggregates in Nafion. The FESEM image in Fig. 3d clearly shows a uniform dispersion of CdSe particles and relatively big size of SPAN aggregates in Nafion. The observations from the OM images were consistent with those from the FESEM images.

Electrochemical properties
of the Nafion/CdSe/SPAN-modified GCE

Figure 4 shows CV curves recorded at various modified GCE in 2 mM DA aqueous solution of pH 7. The anodic peak for the oxidation of DA appeared at near 0.4 V as recorded at the bare GCE. The Nafion/GCE and Nafion/SPAN/GCE enhanced the anodic peak current for DA but shifted the peak to a higher potential at near 0.55 V, an indication that Nafion alone or the Nafion/SPAN composite both electrocatalyzed the oxidation reactions of DA. The Nafion/CdSe/GCE enhanced the anodic peak current even higher than the Nafion/GCE, an indication that CdSe exhibited high electrocatalytic activity to the oxidation of DA. The Nafion/CdSe/SPAN/GCE enhanced the anodic peak current not much higher than the Nafion/CdSe/GCE, an indication that CdSe and SPAN exhibited insignificant synergistic effects on the oxidation reactions of DA.

Figure 5 shows CV curves recorded at various modified GCE in 2 mM UA aqueous solution of pH 7. The anodic peak for the oxidation of UA appeared at near 0.5 V as recorded at the bare GCE. The Nafion/GCE and Nafion/SPAN/GCE exhibited no electrocatalytic activity for the oxidation of UA because of very low anodic currents. The Nafion/CdSe/GCE and the Nafion/CdSe/SPAN/GCE both exhibited low electrocatalytic activity because the two modified GCE did not exhibit higher anodic currents than the bare GCE. Figure 6 shows CV curves recorded at various modified GCE in 2 mM AA aqueous solution of pH 7. The anodic peak for the oxidation of AA appeared at near 0.5 V as recorded at the bare GCE. The four modified GCE all exhibited no electro-catalytic activity to the oxidations of AA because the anodic

Fig. 3 OM and FESEM images of **a** COOH-capped CdSe powders, **b** Nafion/CdSe cast film, **c** Nafion/SPAN cast film, and **d** Nafion/CdSe/SPAN cast film
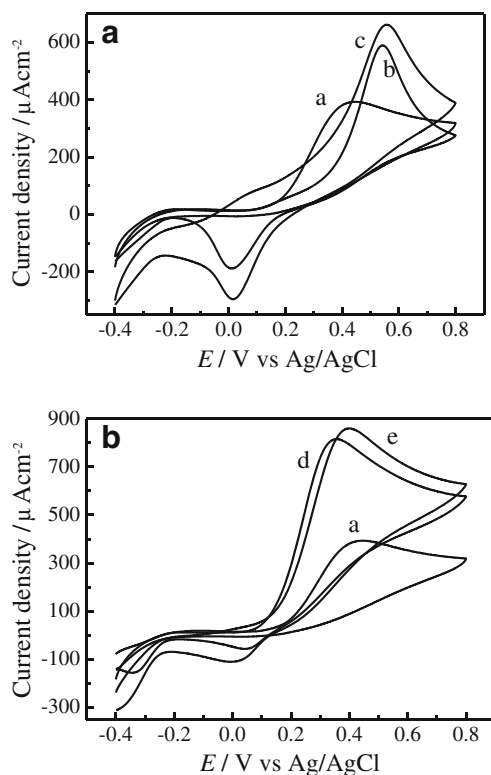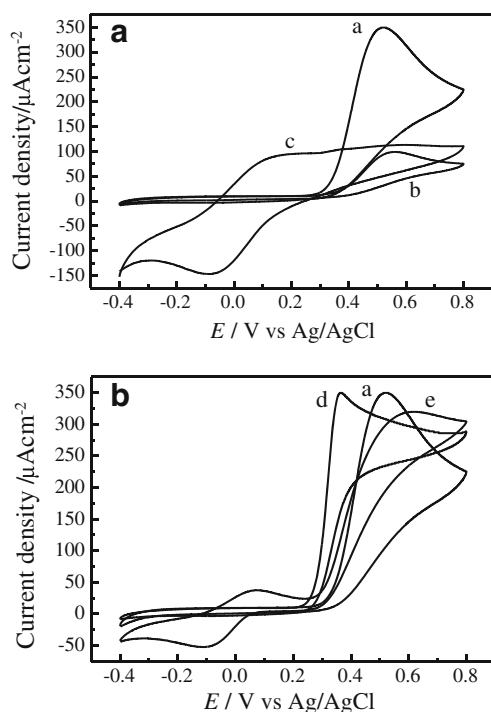
Fig. 4 CV curves recorded at **a** bare GCE, **b** Nafion/GCE, **c** Nafion/SPAN/GCE, **d** Nafion/CdSe/GCE, and **e** Nafion/CdSe/SPAN/GCE in 2 mM DA aqueous solution in the phosphate buffer solution (*PBS*) of pH 7. Scan rate 50 mV/s
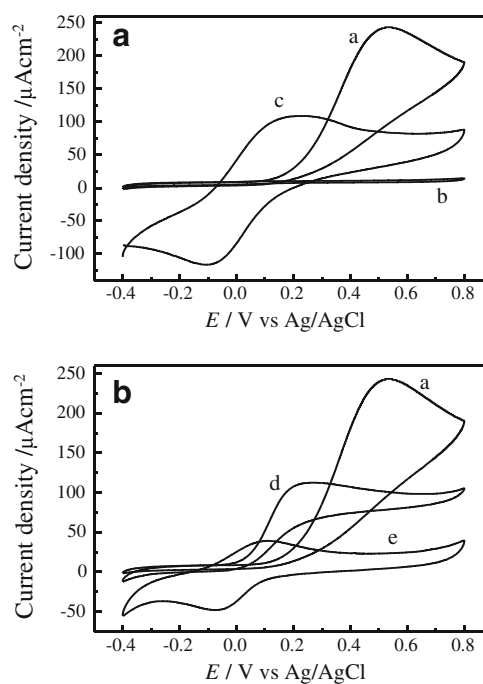

Fig. 5 CV curves recorded at **a** bare GCE, **b** Nafion/GCE, **c** Nafion/SPAN/GCE, **d** Nafion/CdSe/GCE, and **e** Nafion/CdSe/SPAN/GCE in 2 mM UA aqueous solution in PBS of pH 7. Scan rate, 50 mV/s


Fig. 6 CV curves recorded at **a** bare GCE, **b** Nafion/GCE, **c** Nafion/SPAN/GCE, **d** Nafion/CdSe/GCE, and **e** Nafion/CdSe/SPAN/GCE in 2 mM AA aqueous solution in PBS of pH 7. Scan rate, 50 mV/s

peak currents recorded at the four modified GCE were all much lower than the bare GCE.

The observations from Figs. 4, 5 and 6 can be explained by the interactions between the modified GCE and the individual analyte. As schematically presented in Fig. 7, at pH 7, DA was positively charged because pK_a of DA is 8.89 so that DA has strong attractive interactions with the negatively charged sulfonated Nafion, sulfonated SPAN, and carboxylated CdSe, leading to the appearance of the electrocatalytic activity of Nafion, CdSe, and SPAN to the oxidations of DA as can be seen in Fig. 4. UA has a pK_a of 5.4 and thus has a low level of negatively charged anions at pH 7 so that weak repulsive interactions were present between UA with the Nafion/GCE, and with the Nafion/SPAN/GCE, leading these two modified
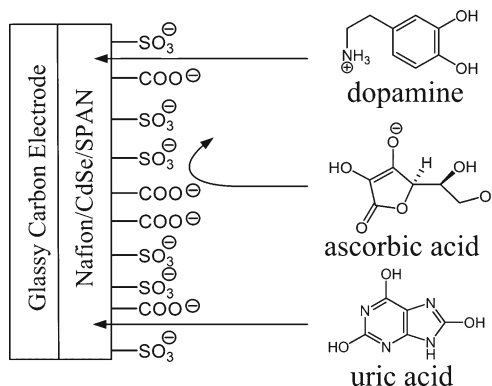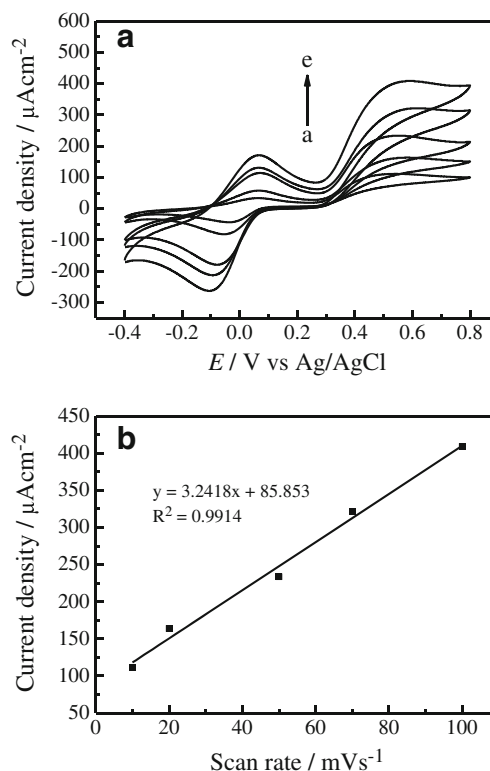

Fig. 7 Schematic presentation of interactions between the surface of the Nafion/CdSe/SPAN/GCE and the three analytes in PBS of pH 7

GCE to no electrocatalytic activity to oxidations of UA (Fig. 5). The incorporation of CdSe into the two modified GCE exhibited an increased anodic peak current of UA, an indication that CdSe was able to electrocatalyze the oxidations of UA. AA has a pK_a of 4.1 and thus has a relatively high level of negatively charged anions at pH 7 so that repulsive interactions were strong between AA and any of the four modified GCE which were all negatively charged, leading to no or very low eletrocatalytic activity of the modified GCE to the oxidations of AA (Fig. 6). The evidence of strong repulsions can be also clearly seen in curve b of Fig. 6, where negligible current was recorded by the Nafion modified GCE in AA aqueous solution of pH 7. The CdSe and SPAN in the Nafion matrix which had strongly repulsive interaction with AA were seen to exhibit low anodic currents (curves c and d of Fig. 6), an indication that CdSe and SPAN had low electrocatalytic ability for the oxidation of AA. CdSe and SPAN had, however, no synergistic effects on the oxidation of AA (curve e of Fig. 6).

Figures 8a and 9a show the variations of CV curves recorded at Nafion/CdSe/SPAN/GCE with scan rates. If the anodic peak current densities are linearly a function of the square root of the potential scan rate, the electron transfer rate on the modified electrode during the oxidations of an analyte is controlled by the diffusion step [43, 44]. If the anodic peak current densities are linearly a function of the potential scan
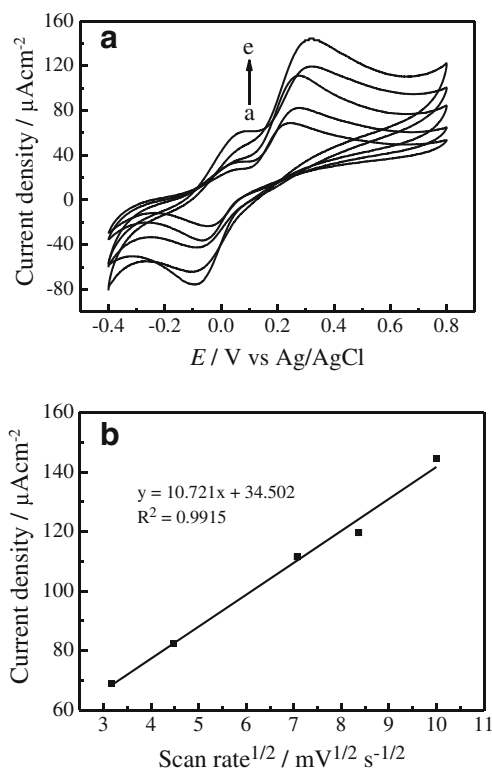
Fig. 9 a CV curves of various scan rates recorded at Nafion/CdSe/SPAN/GCE in 0.8 mM UA of pH 7. b The anodic peak current density at near 0.55 V in a as plotted versus the scan rate. Scan rates (a) 10, (b) 20, (c) 50, (d) 70, and (e) 100 mV/s

rate, the electron transfer rate on the modified electrode during the oxidations of the analyte is controlled by the surface adsorption step [43, 44]. Figure 8b shows linear relationship between the anodic peak current densities of DA and the square root of potential scan rates as recorded at Nafion/CdSe/SPAN/GCE, indicating that the oxidation rate of DA was in a diffusion-controlled process, whereas in Fig. 9b the linear relationship found for UA was between the anodic peak current densities and the potential scan rates, indicating that the oxidation rate of UA was in a surface adsorption-controlled process. The findings from Figs. 8 and 9 were consistent with the previous discussion on the extent of interaction between the modified GCE and DA, and that between the modified GCE and UA. The strong attractive interaction that was present between the modified GCE and DA at pH 7, as discussed previously, would result in a faster rate in the surface adsorption than in the film diffusion during oxidations of DA. The overall oxidation rate of DA was therefore in a diffusion-controlled process, as confirmed in Fig. 8b. The weak repulsive interaction that was present between the modified GCE and UA at pH 7 would result in a slower rate in the surface adsorption than in the film diffusion during oxidations of UA. The overall oxidation rate of UA was thus in a surface adsorption-controlled process, as confirmed in Fig. 9b.

Fig. 8 a CV curves of various scan rates recorded at Nafion/CdSe/SPAN/GCE in 0.2 mM DA of pH 7. b The anodic peak current density at near 0.3 V in a as plotted versus the square root of scan rate. Scan rates (a) 10, (b) 20, (c) 50, (d) 70, and (e) 100 mV/s

In addition, to confirm that the interactions between the modified GCE and the analytes played an important role in the detections of the analytes, the effects of basic media of pH 12 in which the analytes were dissolved on the anodic peak currents of analytes were investigated by CV recorded at Nafion/CdSe/SPAN/GCE. Although we did not show these CV curves in this paper, we found no redox signals at all for DA which was found to exhibit strong anodic peak current in PBS of pH 7 as shown in Fig. 4. This can be attributed to deprotonations of the phenols in DA at pH 12 resulting in negatively charged DA and repulsive interactions with the modified GCE.

Electrochemical properties of the Nafion-pH/CdSe/SPAN modified GCE

Figure 10 shows the FESEM images for the Nafion-2/CdSe/SPAN, Nafion-7/CdSe/SPAN, and Nafion-12/CdSe/SPAN films which were cast from the Nafion/CdSe/SPAN solutions
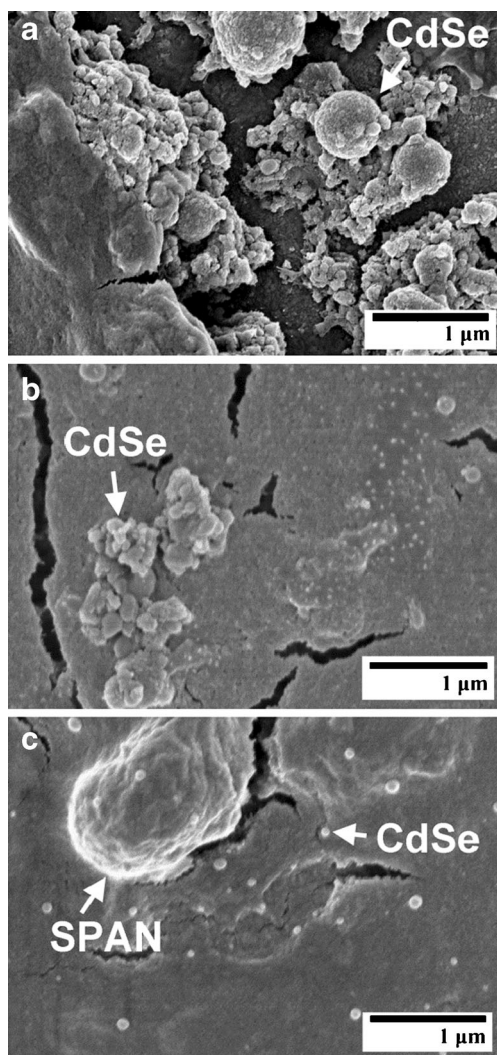
Fig. 10 FESEM images of **a** Nafion-2/CdSe/SPAN, **b** Nafion-7/CdSe/SPAN, and **c** Nafion-12/CdSe/SPAN cast films

of pH 2, 7, and 12, respectively. As can be seen in Fig. 10a, the Nafion-2/CdSe/SPAN film cast from the solution of pH 2 was brittle and exhibited significant phase separation. The visual observation that CdSe was poorly dispersed in the solution of pH 2 prior to casting suggested that the COOH-capped CdSe colloids had coagulated in the solution and were separated by the sulfonated Nafion and SPAN, leading to phase separation in the cast film. In Fig. 10b, Nafion-7/CdSe/SPAN film, as cast from the solution of pH 7, exhibited a decreased CdSe phase separation in the cast film due to the improved CdSe dispersion in the colloidal solution. In Fig. 10c, Nafion-12/CdSe/SPAN film, as cast from the solution of pH 12, exhibited uniform CdSe dispersion in the cast film due to the homogeneous CdSe dispersion in the colloidal solution as can be visually observed on the colloidal solution before casting. Figure 10c suggests that the COOH groups surrounding the CdSe colloids had become negatively charged due to the production of carboxylate anions (COO^-) at pH 12 and the repulsive interactions among the anions had led to homogeneous dispersion in the colloidal solution and thus uniform CdSe dispersion in the cast film.

Figure 11 shows the CV curves for DA, UA, and AA solutions of pH 7 as recorded at the Nafion-pH/CdSe/SPAN/GCE. In curve d of Fig. 11a, the anodic and cathodic peaks at near 0.1 and −0.05 V, respectively, recorded at the Nafion-12/CdSe/SPAN/GCE can be assigned to oxidation and reduction reactions of SPAN. The Nafion-12/CdSe/SPAN/GCE appeared to have much higher anodic and cathodic currents than the Nafion-2/CdSe/SPAN/GCE and Nafion-7/CdSe/SPAN/GCE in Fig. 11a. This indicates that the homogeneity of the cast film helped enhance redox reactions of SPAN on the modified GCE, since the cast film of the Nafion-12/CdSe/SPAN exhibited the better dispersion than that of the Nafion-7/CdSe/SPAN and of the Nafion-2/CdSe/SPAN according to Fig. 10. In curve d of Fig. 11b, in addition to the peak at near 0.1 V for oxidation reaction of SPAN, the Nafion-12/CdSe/SPAN/GCE gave an anodic peak at near 0.38 V which can be assigned to the oxidation reaction of DA based on the observation in curve e of Fig. 4 where the anodic peak appeared at near 0.38 V for DA. The homogeneity of the cast film was found to enhance the electrocatalytic activity of the modified GCE to the oxidation reactions of DA since the Nafion-12/CdSe/SPAN/GCE exhibited much higher anodic peak currents for DA than the Nafion-7/CdSe/SPAN and the Nafion-2/CdSe/SPAN as can be seen in Fig. 11b, in addition to the more negatively charged surface of the film as cast at higher pH to result in stronger ionic interactions with DA as discussed earlier. In curve d of Fig. 11c, in addition to the peak at near 0.05 V for oxidation reaction of SPAN, the Nafion-12/CdSe/SPAN/GCE gave an anodic peak at near 0.58 V which can be assigned to the oxidation reaction of UA based on the observation in curve e of Fig. 5 where the anodic peak appeared at near 0.6 V for UA. The homogeneity
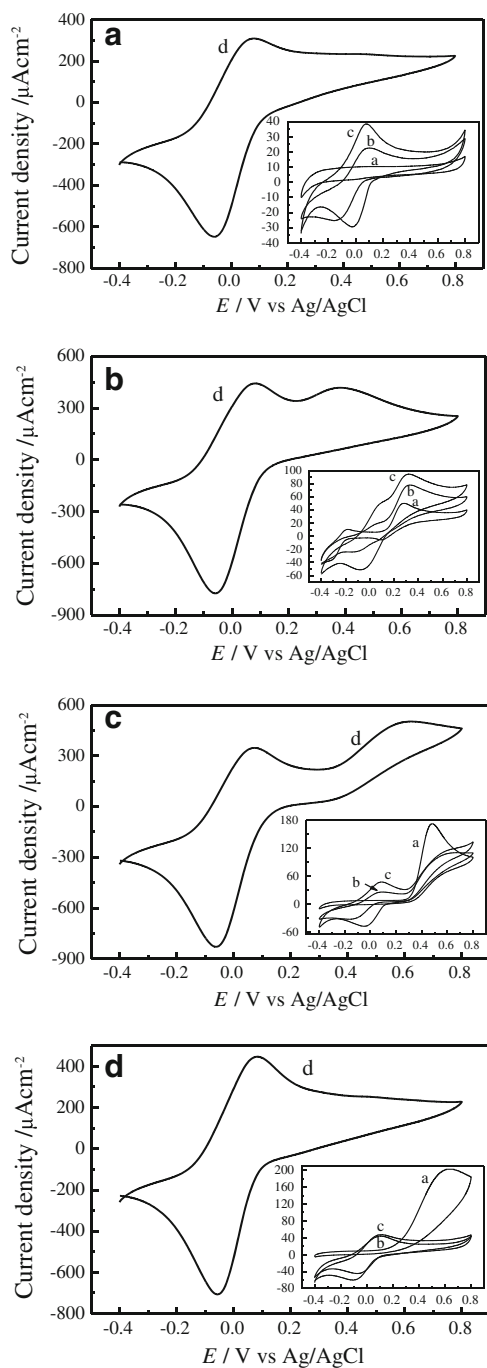
Fig. 11 CV curves recorded at (*a*) bare GCE and at Nafion-pH/CdSe/SPAN/GCE, which were cast from solutions of (*b*) pH 2, (*c*) pH 7, and (*d*) pH 12, in PBS of pH 7 containing **a** control, **b** 0.2 mM DA, **c** 0.8 mM UA, and **d** 1 mM AA. Scan rate, 50 mV/s

of the cast film also played an important factor in the electrocatalytic activity for the oxidation reactions of UA since the Nafion-12/CdSe/SPAN/GCE exhibited much higher anodic peak currents for UA than the Nafion-7/CdSe/SPAN and the Nafion-2/CdSe/SPAN as can be seen in Fig. 11c. In Fig. 11d, the Nafion-12/CdSe/SPAN/GCE exhibited the only anodic peak at near 0.1 V for SPAN without an anodic peak for AA which could occur at near 0.5 V as recorded at bare GCE as

shown in curve a in Figs. 6 and 11d. Figure 11d clearly shows that all three Nafion-pH/CdSe/SPAN/GCE as cast from solutions of three pHs exhibited no anodic peak of AA. This indicates that an increase in homogeneity of the cast film on GCE was not able to change the incapable detection of AA by the Nafion/CdSe/SPAN/GCE to the capable detection by the Nafion-pH/CdSe/SPAN/GCE.

The solution of higher pH (pH 12) gave also the better dispersion in the individual Nafion-pH/CdSe and Nafion-pH/SPAN colloidal solution and thus the higher anodic peak current for the Nafion-pH/CdSe/GCE and Nafion-pH/SPAN/GCE (see Fig. S1), although Nafion-2/SPAN/GCE was slightly higher than Nafion-7/SPAN/GCE. Without the presence of SPAN, the anodic peak of DA appeared at near 0.2 V (Fig. S1a); with the presence of SPAN, the anodic peak of DA appeared at near 0.45 V (Fig. S1b). The characteristic anodic peak of SPAN at near 0.05 V that was observed for the Nafion-12/SPAN/GCE disappeared for the Nafion-2/SPAN/GCE and Nafion-7/SPAN/GCE. This can be perhaps attributed to the less doping effect by the sulfonated Nafion (as a dopant for SPAN) at pH 2 than at pH 7.

The incorporation of CdSe into Nafion-12/SPAN did not give much an increase in the anodic peak current for DA (see Fig. S2), an indication that CdSe and SPAN did not exhibit much synergistic effects on the oxidations of DA, agreeing with the observation in Fig. 4. The anodic peaks at near 0.1 V were characteristic oxidation peaks for SPAN (curves a and b in Fig. S2b) while the anodic peak at near 0.5 V corresponded to the oxidation of UA (curve d in Fig. S2b). The Nafion-12/CdSe/GCE and the Nafion-12/SPAN/GCE both exhibited enhanced anodic peak currents at near 0.5 V, indicating that both modified GCE were able to electrocatalyze the oxidations of UA. The Nafion-12/CdSe/SPAN/GCE enhanced the electrocatalytic activity even higher, an indication that CdSe and SPAN exhibited much synergistic effects on the oxidations of UA. This synergistic effect was not seen when the modified GCE was prepared at low pH as can be seen in Fig. 5.

Conclusions

CdSe and SPAN were dispersed in a commercially available Nafion solution to prepare the Nafion/CdSe/SPAN-modified GCE for the detection of DA, UA, and AA. CV curves have found that the Nafion/CdSe/SPAN/GCE exhibited the highest electrocatalytic activity to oxidations of DA and the least activity to oxidations of AA, in solution of pH 7. This could be attributed to strong attractive interactions between the modified GCE and DA, weak repulsive attractions between the modified GCE and UA, and strong repulsive interactions between the modified GCE and AA. The findings that the oxidations of DA followed a diffusion-controlled process and the oxidations of UA followed a surface adsorption-controlled

process were consistent with the attributed interactions between the modified GCE and the analytes. If cast at a higher pH, the composite was found to exhibit better CdSe and SPAN dispersions in the cast films and higher electrocatalytic activities. CdSe and SPAN exhibited insignificant synergistic effects on the oxidations of DA as cast from solutions of both low and high pHs, whereas CdSe and SPAN exhibited significant synergistic effects on the oxidations of UA as cast from a solution of high pH at 12.

References

1. Li CY, Cai YJ, Yang CH, Wu CH, Wei Y, Wen TC, Wang TL, Shieh YT, Lin WC, Chen WJ (2011) Highly sensitive and selective electrochemical determination of dopamine and ascorbic acid at Ag/Ag$_2$S modified electrode. Electrochim Acta 56:1955–1959

2. Zare HR, Rajabzadeh N, Nasirizadeh N, Mazloum AM (2006) Voltammetric studies of an oracet blue modified glassy carbon electrode and its application for the simultaneous determination of dopamine, ascorbic acid and uric acid. J Electroanal Chem 589:60–69

3. Safavi A, Maleki N, Moradlou O, Tajabadi F (2006) Simultaneous determination of dopamine, ascorbic acid, and uric acid using carbon ionic liquid electrode. Anal Biochem 359:224–229

4. Zhao Y, Gao Y, Zhan D, Liu H, Zhao Q, Kou Y, Shao Y, Li M, Zhuang Q, Zhu Z (2005) Selective detection of dopamine in the presence of ascorbic acid and uric acid by a carbon nanotubes–ionic liquid gel modified electrode. Talanta 66:51–57

5. Aguilar R, Davila MM, Elizalde MP, Mattusch J, Wennrich R (2004) Capability of a carbon–polyvinylchloride composite electrode for the detection of dopamine, ascorbic acid and uric acid. Electrochim Acta 49:851–859

6. Wang HS, Li TH, Jia WL, Xu HY (2006) Highly selective and sensitive determination of dopamine using a Nafion/carbon nanotubes coated poly(3-methylthiophene) modified electrode. Biosens Bioelectron 22:664–669

7. Selvaraju T, Ramaraj R (2003) Simultaneous determination of ascorbic acid, dopamine and serotonin at poly(phenosafranine) modified electrode. Electrochem Commun 5:667–672

8. Li Y, Lin X (2006) Simultaneous electroanalysis of dopamine, ascorbic acid and uric acid by poly(vinyl alcohol) covalently modified glassy carbon electrode. Sensors Actuators B 115:134–139

9. Liu A, Honma I, Zhou H (2007) Simultaneous voltammetric detection of dopamine and uric acid at their physiological level in the presence of ascorbic acid using poly(acrylic acid)-multiwalled carbon–nanotube composite-covered glassy-carbon electrode. Biosens Bioelectron 23:74–80

10. Zhang L, Shi Z, Lang Q (2011) Fabrication of poly(orthanilic acid)–multiwalled carbon nanotubes composite film-modified glassy carbon electrode and its use for the simultaneous determination of uric acid and dopamine in the presence of ascorbic acid. J Solid State Electrochem 15:801–809

11. Yang S, Li G, Yang R, Xia M, Qu L (2011) Simultaneous voltammetric detection of dopamine and uric acid in the presence of high concentration of ascorbic acid using multi-walled carbon nanotubes with methylene blue composite film-modified electrode. J Solid State Electrochem 15:1909–1918

12. Li G, Yang S, Qu L, Yang R, Li J (2011) Simultaneous voltammetric determination of ascorbic acid and uric acid using a Nafion/multi-wall carbon nanotubes composite film-modified electrode. J Solid State Electrochem 15:161–166

13. Zhou Y, He M, Huang C, Dong S, Zheng J (2012) A novel and simple biosensor based on poly(indoleacetic acid) film and its application for simultaneous electrochemical determination of dopamine and epinephrine in the presence of ascorbic acid. J Solid State Electrochem 16:2203–2210

14. Tsierkezos NG, Ritter U (2012) Oxidation of dopamine on multi-walled carbon nanotubes. J Solid State Electrochem 16:2217–2226

15. Shieh YT, Chen YA, Lin RH, Wang TL, Yang CH (2012) Temperature effects on electrocatalytic activities of carbon nanotubes/poly(N-isopropylacrylamide) composites. Electrochim Acta 76:518–525

16. Shieh YT, Chen YA, Lin RH, Wang TL, Yang CH (2012) Temperature responsive carbon nanotubes/poly(N-isopropylacrylamide)-modified electrodes for electrochemical selective determination of dopamine, uric acid, and ascorbic acid. Colloid Polym Sci 290:1451–1456

17. Gerard M, Chaubey A, Malhotra BD (2002) Application of conducting polymers to biosensors. Biosens Bioelectron 17:345–359

18. Tatsuma T, Ogawa T, Sato R, Oyama N (2001) Peroxidase-incorporated sulfonated polyaniline–polycation complexes for electrochemical sensing of H$_2$O$_2$. J Electroanal Chem 501:180–185

19. Zhu N, Chang Z, He P, Fang Y (2006) Electrochemically fabricated polyaniline nanowire-modified electrode for voltammetric detection of DNA hybridization. Electrochim Acta 51:3758–3762

20. Slim C, Ktari N, Cakara D, Kanoufi F, Combellas C (2008) Polyaniline films based ultramicroelectrodes sensitive to pH. J Electroanal Chem 612:53–62

21. Prakash S, Rao CRK, Vijayan M (2009) Polyaniline–polyelectrolyte–gold(0) ternary nanocomposites: synthesis and electrochemical properties. Electrochim Acta 54:5919–5927

22. Bian LJ, Zhang JH, Qi J, Liu XX, Dermot D, Lau KT (2010) Immobilization of molybdenum oxide in polyaniline and electrocatalytic properties of the composite modified electrode. Sensors Actuators B 147:73–77

23. Shieh YT, Jung JJ, Lin RH, Yang CH, Wang TL (2012) Electrocatalytic behavior of carbon nanotubes in electropolymerizations of self-doped polyaniline used as a sensing material. J Electrochem Soc 159:H921–H927

24. Shieh YT, Jung JJ, Lin RH, Yang CH, Wang TL (2012) Electrocatalytic activity of self-doped polyaniline. Electrochim Acta 70:331–337

25. Sanghavi BJ, Srivastava AK (2010) Simultaneous voltammetric determination of acetaminophen, aspirin and caffeine using an in situ surfactant-modified multiwalled carbon nanotube paste electrode. Electrochim Acta 55:8638–8648

26. Sanghavi BJ, Srivastava AK (2011) Adsorptive stripping differential pulse voltammetric determination of venlafaxine and desvenlafaxine employing Nafion–carbon nanotube composite glassy carbon electrode. Electrochim Acta 56:4188–4196

27. Sanghavi BJ, Hirsch G, Karna SP, Srivastava AK (2012) Potentiometric stripping analysis of methyl and ethyl parathion employing carbon nanoparticles and halloysite nanoclay modified carbon paste electrode. Anal Chim Acta 735:37–45

28. Salinas-Torres D, Huerta F, Montilla F, Morallon E (2011) Study on electroactive and electrocatalytic surfaces of single walled carbon nanotube-modified electrodes. Electrochim Acta 56:2464–2470

29. Guo W, Xu L, Li F, Xu B, Yang Y, Liu S, Sun Z (2010) Chitosan-assisted fabrication and electrocatalytic activity of the composite film

electrode of heteropolytungstate/carbon nanotubes. Electrochim Acta 55:1523–1527

30. Pang HL, Liu J, Hu D, Zhang XH, Chen JH (2010) Immobilization of laccase onto 1-aminopyrene functionalized carbon nanotubes and their electrocatalytic activity for oxygen reduction. Electrochim Acta 55:6611–6616

31. Shieh YT, Yu TY, Wang TL, Yang CH (2012) Effects of pH on electrocatalytic activity of carbon nanotubes in polyethylenimine composites. J Electroanal Chem 664:139–145

32. Shieh YT, Yu TY, Wang TL, Yang CH, Liao WT (2012) Effects of pH on electrocatalytic activity of functionalized carbon nanotubes. Colloid Polym Sci 290:1–9

33. Rivas GA, Rubianes MD, Rodrıguez MC, Ferreyra NF, Luque GL, Pedano ML, Miscoria SA, Parrado C (2007) Carbon nanotubes for electrochemical biosensing. Talanta 74:291–307

34. Gao F, Yin J, Yao Z, Li M, Wang L (2010) A nanocomposite modified electrode: electrocatalytic properties and its sensing applications to hydrogen peroxide and glucose. J Electrochem Soc 157: F35–F39

35. Henstridge MC, Dickinson EJF, Aslanoglu M, Batchelor-McAuley C, Compton RG (2010) Voltammetric selectivity conferred by the modification of electrodes using conductive porous layers or films: the oxidation of dopamine on glassy carbon electrodes modified with multiwalled carbon nanotubes. Sensors Actuators B 145:417–427

36. Kozub BR, Rees NV, Compton RG (2010) Electrochemical determination of nitrite at a bare glassy carbon electrode; why chemically modify electrodes? Sensors Actuators B 143:539–546

37. Streeter I, Wildgoose GG, Shao L, Compton RG (2008) Cyclic voltammetry on electrode surfaces covered with porous layers: an analysis of electron transfer kinetics at single-walled carbon nanotube modified electrodes. Sensors Actuators B 133:462–466

38. Huang CP, Liu SW, Chen TM, Li YK (2008) A new approach for quantitative determination of glucose by using CdSe/ZnS quantum dots. Sensors Actuator B 130:338–342

39. Brus L (1986) Electronic wave functions in semiconductor clusters: experiment and theory. J Phys Chem 90:2555–2560

40. Tauc J (1974) Amorphous and liquid semiconductors. Plenum, New York

41. Baskoutas S, Terzisa AF (2006) Size-dependent band gap of colloidal quantum dots. J Appl Phys 99:013708

42. Chen SA, Hwang GW (1996) Structure characterization of self-acid-doped sulfonic acid ring-substituted polyaniline in its aqueous solutions and as solid film. Macromolecules 29:3950–3955

43. Bard AJ, Faulkner LR (2001) Electrochemical methods: fundamentals and applications, 2nd edn. John Wiley & Sons, New York

44. Bergren AJ, Porter MD (2006) The characteristics of selective heterogeneous electron transfer for optimization of redox recycling amplification systems. J Electroanal Chem 591:189–200